

# Wave Effects on Multiple Bodies

J. N. NEWMAN

Massachusetts Institute of Technology  
Cambridge, MA 02139, USA

## Abstract

Significant hydrodynamic interactions occur when bodies are located in close proximity on the ocean surface. This situation exists in many applications of practical importance, which require rational engineering analyses. Solutions based on panel methods and other direct numerical methods can be used for configurations involving relatively small numbers of bodies. When the number of bodies is very large, asymptotic approximations are required. This paper reviews the extensive analytical and numerical accomplishments in this field. New computations are included to illustrate first- and second-order interaction effects. Special consideration is given to configurations where the interactions are singular at certain frequencies.

## 1. Introduction

Many applications occur in the field of marine hydrodynamics where two or more vessels are in sufficiently close proximity to experience significant interactions. Catamarans and other multi-hull ships, offshore platforms supported by multiple columns, floating bridges, and arrays of wave-power devices are all examples where the proximity is a permanent feature of the design. In other cases, such as marine operations involving multiple vessels and platforms or replenishment operations of two ships, the proximity is temporary but nevertheless important. Hydrodynamic interactions related to wave effects are particularly significant, due to the oscillatory phase of the waves in relation to the spacing, and the large horizontal scale of the wave influence.

Multiple bodies can be studied with the same experimental and theoretical methods that are applied to wave effects on a single body. Typically, the analysis of two or three interacting bodies is a straightforward extension, but the analysis of very large configurations is fundamentally more difficult. On the experimental side, the physical size of the model may exceed the practical limits of the wave basin, and the sensitivity of the response to the wave period and direction may dictate an extensive series of tests. Thus there is a great need for reliable theories and associated computational tools suitable for analyzing these problems. Moreover, the variety of interesting interactions that occur for multiple bodies provides a rich source of stimulus for fundamental research.

In most cases of practical importance, the effects of ocean waves on floating and submerged bodies can be analyzed by the linear potential theory. This theory is well established for fixed structures, and for vessels which have no substantial forward velocity. Classical solutions exist for relatively simple body shapes such as circular cylinders. In some cases it is necessary to account for second-order effects, including mean drift forces and more complex time-varying nonlinearities. The same fundamental theory can be extended to the analysis of wave effects on multiple bodies. In some of the examples cited above the different bodies are connected structurally, and in others they are dynamically independent. The distinction between structurally connected or independent bodies is not important from the hydrodynamic standpoint, except insofar as the total number of modes of body motion is reduced if the connections are rigid.

Much recent attention has been devoted to ‘Very Large Floating Structures’ (VLFS) suitable for use as floating airports and ‘Mobile Offshore Bases’ (MOB). On the order of  $10^4$  separate buoyancy elements are used in some of the proposed designs for floating airports. Typical MOB designs involve joining several large semi-submersibles with flexible connectors which permit rotational deflections between the vessels. Among the challenging technical issues for this type of structure is the coupling and decoupling of the vessels in a seaway. A similar issue exists for the pontoon-type of VLFS, an array of rectangular shallow barges which are joined together in the water.

The complexity of multi-body solutions increase rapidly with the number of elements. To meet this challenge there has been steady progress in the development of numerical methods which extend the capabilities of direct-solution techniques, including panel methods suitable for the analysis of arbitrary structures and special multipole methods suitable for arrays of vertical cylinders and other axisymmetric elements. To complement these direct solutions, and offer computationally feasible alternatives for very large arrays, approximations have been developed which are based in varying degrees on the hydrodynamic properties of infinite arrays.

A brief historical review of this subject is presented in Section 2, with special attention given to the seminal works of Professor Makoto Ohkusu. The theoretical formulation is outlined in Section 3, with emphasis on techniques for representing the various radiation modes in a computationally efficient and general form. Section 4 describes two examples of drift forces on multiple bodies, one the slow oscillations of two independent bodies and the other the drift force on individual elements of a large array. Periodic arrays of bodies which extend to infinity, and the analogous problems of bodies in channels, are considered in Section 5. Closely related work on finite arrays is described in Section 6, with emphasis on the phenomenon of near-trapping. In Section 7 the extension to second-order second-harmonic effects is reviewed, with a comparison made between different models for a tension-leg platform (TLP). Section 8 describes recent work on doubly-infinite periodic arrays, and their relation to large rectangular finite arrays such as the column-supported VLFS. Conclusions are summarized in Section 9.

## 2. History

One of the first papers on this topic was published in 1969 by Ohkusu [44]. He extended the classical solution for a single heaving circular cylinder, first developed by Ursell [55], to the case of two cylinders in a catamaran configuration. This type of two-dimensional analysis is most relevant to the interactions between adjacent ship hulls in beam seas. Such interactions are particularly strong, indeed nearly singular, when the spacing between the hulls is an integer multiple of half a wavelength. More extensive computations and experiments were published in a subsequent paper [45] and a subset of these results is included in a more recent survey [50].

Motivated by practical designs for offshore platforms with multiple columns, Ohkusu [46] also developed a three-dimensional technique using the eigenfunction expansions for single axisymmetric cylinders to account for their mutual wave interactions. His first paper presented at an international symposium [47] summarized and extended both of these pioneering contributions, and brought his work to the attention of the international community. Coincidentally, the Proceedings of that symposium include on adjoining pages one of the first papers devoted to the direct numerical solution of wave effects on three-dimensional floating bodies, by Faltinsen and Michelsen [15]. That panel method was extended subsequently to analyze two independent bodies by van Oortmerssen [52, 53] and Løken [31], but the computational resources of that time restricted their work to simple body shapes represented by rather large panels.

Second-order slowly-varying drift forces are particularly important for vessels in close proximity. Over many cycles of the first-order oscillatory motions, the drift forces may cause substantial changes in the relative positions, possibly leading to collisions. Ohkusu [48] demonstrated the importance of hydrodynamic interactions on the drift force. His presentation of that paper included a memorable cinematic record of experiments, showing the behavior in beam seas of a small vessel on the weather side of a larger fixed structure. The sign of the drift force was shown to change depending on the spacing relative to the wavelength. As a result, the drift motion of the smaller vessel oscillated slowly in time. Another illustration of the same phenomenon is presented in Section 4.

Over the years, as computational power has increased and software has been refined, the panel method has been applied to more complex arrays and multi-body configurations. Lee & Newman [26] show results for a proposed MOB consisting of five large semi-subs joined by hinges, with ten columns on each semi-sub. A more extensive hydroelastic analysis of a similar MOB configuration is reported by Kim *et al* [23]. Maniar and Newman [33] present results for the diffraction past an array of 100 vertical cylinders, with emphasis on the phenomenon of near-trapping which is described in Section 6. Accelerated methods, such as those based on the pre-corrected FFT algorithm [24, 40, 42], can extend the computational limits substantially.

The multiple-scattering method is an alternative approach which is particularly efficient for arrays of axisymmetric bodies. It is based on (1) expanding the potential due to each body in cylindrical harmonics, (2) using Graf's addition theorem to transform to the local coordinates of the other cylinders, and (3) solving the generalized scattering problems for each of the other cylinders in the presence of the first. This method, which was introduced to water-wave problems by Ohkusu [47], has been developed and extended by Kagemoto & Yue [17], Linton & Evans [28], Mavrakos [34], and in other works cited by these authors. Accelerated methods also can be used here, as demonstrated by Murai *et al* [39], Kashiwagi [20], and Utsunomiya *et al* [58]. Murai *et al* [39] analyze VLFS structures of the column-supported and pontoon types, as well as hybrid combinations of the two types. For the pontoon type they compute the relative motions between one sub-element barge and the remaining very large structure, with application to the operation of joining the sub-elements in the ocean.

Williams & Li [59] use the multiple-scattering method to analyze arrays of cylinders with porous walls. Chakrabarti [3, 4] has used the multiple-scattering method to represent the interactions between different bodies, in combination with local solutions at each body based on the panel method.

Budal [1] and Falnes [14] have analyzed arrays of small wave-power absorbers, motivated by the economy of building large numbers of small devices, and also by the favorable outputs that could be achieved with optimum spacing of the elements in the array relative to the wavelength. Simplified theories based on long-wavelength and large-spacing approximations were used initially. A summary and comparison of different approximations is given by Mavrakos & McIver [35], together with accurate results based on the multiple-scattering method. McIver & McIver [38] analyze a line of submerged Bristol cylinders with intermediate gaps.

In cases where a very large number of identical buoyancy elements are arranged in a periodic array, it is logical to develop approximations based on the limiting case where the array extends to infinity. Kagemoto *et al* [18] describe approximations for analyzing wave diffraction by long rectangular pontoon-type bodies, and also by large arrays of small columns. Ohkusu and Namba [51] have developed local approximations valid near the edges of a rectangular mat-type structure. A similar approach may be required to analyze the edges of a large periodic array. This topic is discussed more extensively in §8.

### 3. Theoretical formulation

Following the usual conventions, a Cartesian coordinate system  $\mathbf{x} = (x, y, z)$  is used, with  $z = 0$  the equilibrium plane of the free surface and  $z$  positive upwards. Except where otherwise noted we shall simplify the discussion by assuming that the fluid depth is infinite, and that plane incident waves propagate in the  $+x$ -direction with radian frequency  $\omega$  and wavenumber  $K = \omega^2/g$ .

The fluid velocity is defined as the gradient of the velocity potential, which

is expressed in the time-harmonic form as the real part of the complex product  $\phi(\mathbf{x}) e^{i\omega t}$ . The potential  $\phi$  is governed by Laplace's equation in the fluid domain. The linearized free-surface condition  $K\phi - \partial\phi/\partial z = 0$  is applied on  $z = 0$ .

One or more bodies are present in the fluid, either floating on the free surface or submerged. Each body is identified by an index  $k$ , where  $k = 1, 2, \dots, N$  and  $N$  is the total number of bodies. The submerged surface of each body is denoted by  $S_k$  and the global body surface  $S$  is defined by the union of all body surfaces. Except in the special case of porous bodies, the normal components of the body and fluid velocity vectors are equal on  $S$ . The fluid motion vanishes at large depths, and in the far field the radiated waves due to the presence of the bodies must be outgoing.

It is convenient to decompose the potential in the alternative forms

$$\phi = \phi_D + \phi_R = \phi_I + \phi_S + \phi_R. \quad (1)$$

Here  $\phi_D = \phi_I + \phi_S$  is the solution of the diffraction problem where  $\partial\phi_D/\partial n = 0$  on  $S$ ,  $\phi_I$  is the potential of the incident-wave system, and  $\phi_S$  is the scattered field due to the presence of the bodies. The radiation potential  $\phi_R$  represents the fluid disturbance due to the motions of the bodies.

In the simplest case of a single rigid body with six degrees of freedom, it is logical to express the radiation potential in the form

$$\phi_R = i\omega \sum_{j=1}^6 \xi_j \phi_j, \quad (2)$$

where  $\xi_j$  is the complex amplitude of the body motion in each degree of freedom (surge, sway, heave, roll, pitch, yaw). The boundary condition on  $S$  is then expressed in the form

$$\partial\phi_j/\partial n = n_j, \quad (3)$$

where

$$(n_1, n_2, n_3) = \mathbf{n}, \quad (n_4, n_5, n_6) = \mathbf{x} \times \mathbf{n}. \quad (4)$$

The hydrodynamic pressure force (and moment) acting on the body are represented by the exciting-force coefficients

$$X_i = -i\omega\rho \iint_S \phi_D n_i dS, \quad (5)$$

and by the added-mass and damping coefficients

$$A_{ij} - (i/\omega)B_{ij} = \rho \iint_S \phi_j n_i dS. \quad (6)$$

One way to extend this notation if  $N > 1$  bodies are present is to use an additional index to identify each body. Thus the exciting force  $X_i^{(k)}$  acting on body  $k$  is the contribution to the global integral (5) from the surface  $S_k$ , and the radiation potentials due to body  $k$  are defined similarly in the form  $\phi_j^{(k)}$ . With

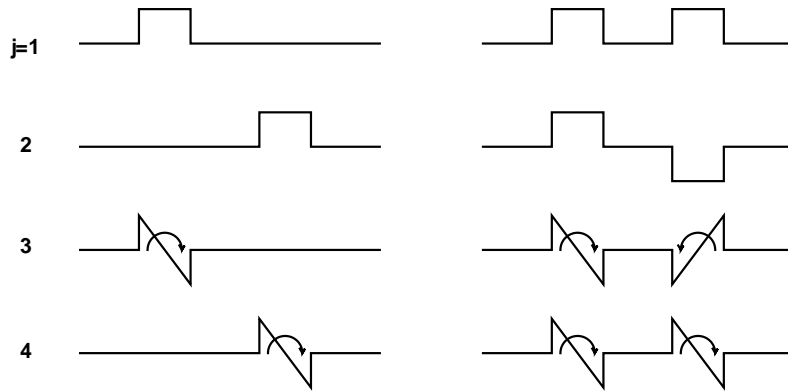


Fig. 1 Physical (left) and generalized (right) modes used to represent the vertical and rotational motions of two bodies, e.g. a catamaran with independent heave and roll motions of each hull. The physical modes are defined separately for each body, with the other body fixed. The generalized modes are defined to be symmetric ( $j$  odd) or antisymmetric ( $j$  even) about the midpoint between the two hulls.

this notation the added-mass and damping coefficients require double-superscripts to distinguish the effects of each body's motions on the others [25]. This facilitates the interpretation of each body's role, and it is most logical in when each body is physically separate from the others.

An alternative and more compact notation follows if the original indices  $(i, j)$  are extended to include all of the relevant separate effects of each body. For two bodies, each having six conventional rigid-body modes, the extended indices  $j = 7, 8, \dots, 12$  are used to define the six modes and force components of the second body. This simplifies the changes required both in the theoretical formulation and in programming. This notation is more logical if the separate bodies are viewed as elements of a single global body with the submerged surface  $S$ , and the various modes  $j$  represent the appropriate modes of normal velocity on this surface. This notation is also useful in its extension to represent generalized modes, as described below.

Generalized modes, also known as generalized coordinates, can be used in various ways [41] to represent the different rigid-body modes of multiple bodies, structural deflections of bodies, and even the motions of interior free surfaces such as moonpools and oscillating water columns. One or more of these physically different extensions can be analyzed simultaneously with a logical framework. For example, Lee & Newman [26] combine hinge deflection modes and bending modes in a single set of generalized-mode shapes suitable for the hydroelastic analysis of five semi-submersibles connected by hinges. If a set of generalized modes  $j = 1, 2, \dots, J$

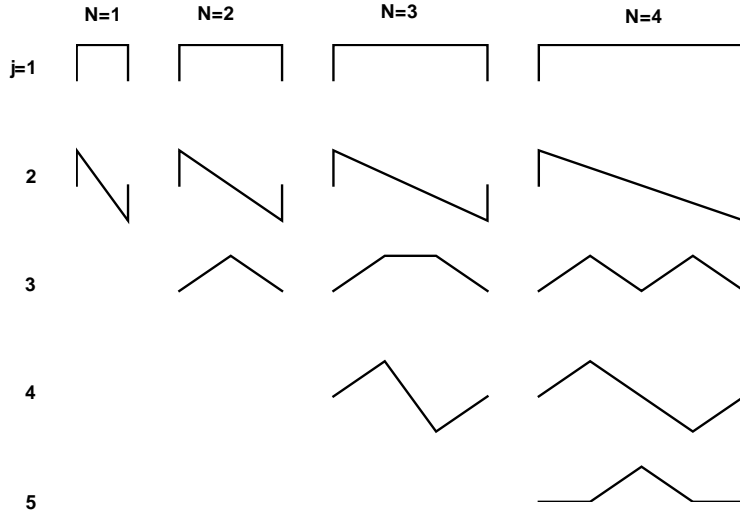


Fig. 2 Generalized modes used to represent the motions of  $N$  identical bodies connected by  $N - 1$  simple hinges. These mode shapes are defined to be either symmetric or antisymmetric about  $x = 0$ . The first two modes correspond to global heave and pitch without hinge deflections. The remaining modes represent the hinge deflections with zero displacement at the ends.

are defined by a corresponding set of generalized normal-velocity components  $n_j$ , no changes are required to extend the definitions of the hydrodynamic force coefficients (5-6). Fundamental properties including symmetry of the added-mass and damping coefficients, and the Haskind relations for the exciting forces, also are unchanged.

It is straightforward to express the conventional rigid-body modes of motion in terms of a different set of generalized modes, or *vice versa*. The use of generalized modes has two computational advantages. Firstly, if the global body surface  $S$  is symmetric about one or more planes of symmetry, the symmetric/antisymmetric components of the radiation potentials can be defined separately in terms of corresponding generalized modes. A simple example with two identical bodies is illustrated in Figure 1. Secondly, if the bodies are connected by structural constraints such as hinges, the number of modes can be reduced and the constraints imposed without special programming changes. Appropriate modes for representing up to four hinged bodies are shown in Figure 2.

#### 4. Drift forces on multiple bodies

As noted in §2, the second-order slowly-varying drift forces are particularly important for vessels in close proximity. In most cases the mean drift force acting on a floating body is in the downwave direction. Thus floating objects, like the wa-

ter particles themselves, drift slowly in the same direction as the incident waves. It is easy to verify this statement for a single body, floating freely on an unbounded free surface. Ohkusu [48] demonstrated a remarkable exception when he analyzed a small ship lying in beam seas near the weather side of a large fixed vessel. The physical explanation for this phenomenon was clear from the cinematic observations of experiments: resonant standing waves occur at critical values of the separation distance between the two vessels, and the resulting radiation stress effectively pushes the two vessels apart.

This phenomenon is obvious in two dimensions, and it can be expected to play an important role in the interactions of ship-like vessels in beam seas, but the existence of a negative drift force is less obvious for three-dimensional configurations which are not elongated parallel to the wave crests. To study this further we consider the same example used by Danmeier [7, 8], where a freely floating hemisphere is upwave of a circular cylinder with vertical axis. The hemisphere and cylinder have the same radius  $a$  and the cylinder draft is  $2a$ . Figure 3 shows how the drift force on the hemisphere depends on the spacing for four different wavenumbers. In long waves, corresponding to the wavelength ratio  $\lambda/a = 10$ , the drift force is relatively small but oscillatory with amplitude much greater than the limiting value when the two bodies are far apart. Since the oscillations diminish slowly with increasing separation distance, there are many intervals of the spacing where the drift force is negative. In shorter waves, e.g.  $\lambda/a = 5$  where the maximum drift force occurs, the sign is always positive. For the intermediate case shown in Figure 3,  $\lambda/a = 6.67$ , both the oscillatory and limiting values are substantial, but only two negative regimes exist.

If the wavelength is not too short, it follows from a quasi-steady analysis that the drift motion of the hemisphere will oscillate slowly in time, moving back and forth between zones of positive and negative drift force in precisely the same manner as in the experiments of Ohkusu [48]. This has been confirmed by Danmeier [7, 8], using a time-domain analysis, but the computational cost of that method limited the duration to slightly less than one oscillatory drift cycle.

For a single body the mean drift force can be evaluated directly, from integration of the second-order pressure on the body surface, or alternatively from momentum conservation. The direct approach is generally more difficult since it requires a higher degree of numerical precision. The difficulties are especially significant for bodies with sharp corners such as truncated cylinders. For multiple bodies it is generally not possible to evaluate the drift force separately for each body from the momentum analysis in the far field. A local momentum analysis has been developed by Ferreira & Lee [16] to overcome this problem, but this approach requires the computation of the fluid velocity and pressure at a large number of control points in the near field.

An interesting example of recent numerical progress in this field is presented by Kashiwagi [22], who computes the local drift force on various elements of an array of 64 truncated circular cylinders. The array includes four rows with 16



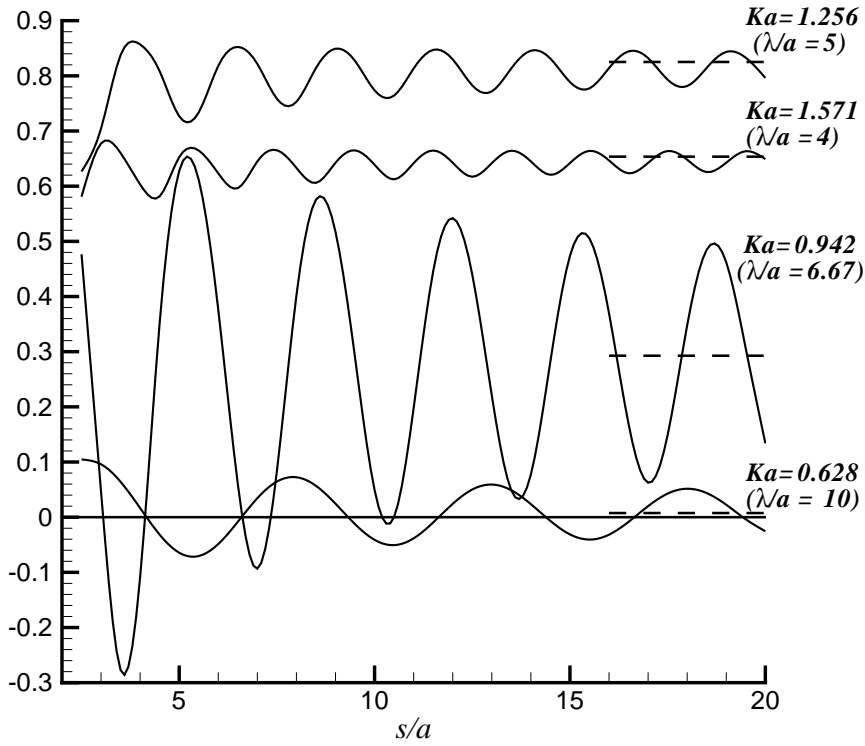


Fig. 3 Mean drift force acting on a freely floating hemisphere upwave of a fixed vertical cylinder, plotted vs. the separation distance  $s$ . The two bodies have the same radius  $a$ , the cylinder draft is  $2a$ , and  $s$  is the distance between their centers. The drift force is normalized by the product  $\rho g a A^2$  where  $\rho$  is the fluid density,  $g$  is gravity, and  $A$  is the incident-wave amplitude. The normalized wavenumber  $Ka$  and wavelength  $\lambda/a$  are shown on the right. The dashed lines show the values of the drift force on the hemisphere alone, or in the limit  $s/a \rightarrow \infty$ .

elements in each row. For cylinders at the upwave end, the drift force oscillates rapidly as a function of the wavenumber below the critical wavenumber where near-trapping occurs (as explained below). Above this wavenumber the upwave elements experience a drift force similar to a single isolated cylinder, but with larger magnitude. Elements in the middle of the array experience a mean drift force which oscillates less rapidly below the critical wavenumber, with a sharp peak at the critical wavenumber, followed by small magnitude above this critical point due to sheltering. The elements near the downwave end of the array experience drift forces which are smaller, or vary more slowly, except near the critical wavenumber where oscillatory features occur. These computations are substantially confirmed by parallel experimental measurements.

## 5. Bodies in channels and infinite periodic arrays

A direct analogy exists between two different problems, (A) a single body in a channel with parallel vertical walls, and (B) a periodic array consisting of the same body and an infinite set of images reflected about the walls. Both problems have practical applications, including the estimation of wall reflection in experiments carried out in narrow wave tanks, and the use of large periodic arrays for the support of piers or bridges and very large floating structures (VLFS). Only (B) can be considered strictly as involving multiple bodies, but the analogy justifies considering the two problems together here.

Ohkusu [49] analyzed the reflection and transmission of waves by a periodic array of vertical circular cylinders, using the eigenfunction expansion for a single cylinder and summing the infinite series for each image. Comparison was made with experimental results for a cylinder in a channel, and also for two cylinders situated with their axes on the channel centerline. The strong dependence on the wavenumber was generally confirmed, with good agreement between the theory and experiments. Singular results were found at the frequency corresponding to the first symmetric transverse standing wave in the channel. No singular results are evident at the lower frequency where an antisymmetric trapped mode might be observed, perhaps because the forcing incident wave system is symmetric.

The existence of trapped modes was established for this class of problems by Callan *et al* [2]. For the case of a single vertical cylinder of radius  $a$  on the centerplane  $y = 0$  of a channel with vertical walls at  $y = \pm d$ , they showed that a nontrivial motion of the fluid and free surface exists with no forcing from incident waves or motions of the cylinder. This solution exists at a particular wavenumber  $K$  in the range  $1.32 < Kd < \pi/2$ , with the precise value dependent on  $a/d$ . Following earlier work on trapped modes along the axis of horizontal cylinders [56], this type of motion is referred to as a ‘trapped mode’ since it is confined to the domain near the (vertical) cylinder and no energy radiation occurs in the far field. The trapped mode discovered by Callan *et al* [2] is antisymmetric about  $y = 0$ . Physically it resembles a localized ‘sloshing mode’ in the channel. However it differs, both in wavenumber and in localization, from the simple transverse standing wave that exists at  $Kd = \pi/2$  in an unobstructed channel.

Other cases of trapping by one or more bodies in a channel have been discovered subsequently by Evans *et al* [9], Evans & Porter [10], McIver *et al* [37], Utsunomiya & Eatock Taylor [57], and Linton & McIver [30]. Closely related works which are relevant to finite arrays are discussed in the following section.

In the references discussed above the bodies are cylindrical throughout the vertical water column, and fixed. In these circumstances the boundary-value problem for the velocity potential can be reduced to a solution of the modified wave equation in the horizontal plane, and direct analogies exist with two-dimensional acoustic problems. The full three-dimensional problem must be considered if the body geometry changes with depth, or if radiation problems are considered. Two

approaches have been used in such cases: (1) superposing a large finite number of images and summing their effects, or (2) using special multipoles or Green functions which satisfy the boundary conditions on the channel walls.

The method based on superposing a finite number of images has the advantage that it can be used with computer codes intended for use with a single compact body, simply by extending the definition of the body to include the images. This method has been criticized, on the basis of slow convergence of the corresponding series for the Green function and incorrect far-field asymptotics, but the convergence of computed local quantities such as the hydrodynamic force coefficients is usually faster. Newman [41] gives illustrative results for the hydrodynamic force coefficients showing the convergence with increasing numbers of images.

The method based on special multipoles which satisfy the boundary conditions on the channel walls has been applied to infinite arrays of truncated circular cylinders by Yeung & Sphaier [60] and Linton & Evans [29]. Linton & Evans devote special efforts to the derivation of integral representations for the multipoles which satisfy exactly the conditions on the channel walls and in the far field. They show the existence of trapped modes for cylinders which are either submerged, extending from the bottom part-way up to the free surface, or surface-piercing and extending part-way down to the bottom. Linton [27] has derived a more efficient representation for the Green function in a channel of finite depth.

## 6. Finite arrays and near-trapping

In work that was intended to test the limits of a higher-order panel method, Maniar & Newman [33] analyzed long arrays with up to 100 vertical cylinders. They discovered that, as the number of cylinders is increased, the local solution in the interior of the array increases without apparent limit in narrow bands of wavenumbers. The locations of these bands are slightly below the values  $Kd = n\pi/2$ , where  $2d$  is the spacing between the axes of adjacent cylinders and  $n = 1, 2, 3, \dots$ . The odd modes ( $n = 1, 3, 5, \dots$ ) have a phase difference of  $180^\circ$  at adjacent elements and zero normal velocity ( $\partial\phi/\partial y = 0$ ) on the vertical planes  $y = \pm d, \pm 3d, \dots$ , corresponding to the channel walls and their images (in the analogous case of a cylinder on the center of a channel). Conversely, the even modes ( $n = 2, 4, 6, \dots$ ) are in phase at adjacent elements and  $\phi = 0$  on the vertical planes  $y = \pm d, \pm 3d, \dots$ . In view of these boundary conditions, the odd/even modes are called Neumann or Dirichlet modes, respectively.

For the first Neumann and Dirichlet modes, Maniar & Newman [33] showed that very large local exciting forces act on the cylinders near the middle of the array (up to 35 times the force on a single cylinder, in the case  $N = 100$ ). The connection with trapped modes was suggested by the coincidence of the first wavenumber ( $n = 1$ ) with the trapped-mode wavenumber reported by Callan *et al* (1991). Since the array is finite, the analogy with trapped modes on infinite arrays (or bodies in channels) is approximate, but with increasing correspondence as the length of the array increases toward infinity. When a distinction is appropriate,

for finite arrays, these modes are referred to as ‘near-trapped’ modes. (The latter term is also used to describe the higher modes  $n > 2$  which are above the cut-off wavenumber in a channel, and hence radiate some energy to the far field.)

Similar results have been found by Evans & Porter [11, 12] for a circular array of  $N$  cylinders. The case  $N = 4$  is particularly important for offshore platforms, although the column radius of practical structures is usually smaller (relative to the spacing) than in the configurations where strong near-trapping effects exist. Other configurations where near-trapping has been demonstrated include rectangular arrays, where the number of these modes is generally increased [12, 20, 43]. Kashiwagi [22] has computed the local drift force on array elements, as discussed in §4. The anti-symmetric trapped mode cannot cause a mean drift force by itself, but the occurrence of singular peaks in [22] may be explained by the quadratic interaction between the trapped mode and the antisymmetric component of the regular solution.

The understanding of near-trapping on long finite arrays has been brought into a clearer focus by Evans & Porter [12], who show that it is closely related to amplitude-modulated Rayleigh-Bloch waves along an infinite array. An illuminating mechanical analogy is described by Utsunomiya & Eatock Taylor [57].

The practical implications of near-trapping have been questioned on various grounds, including nonlinear effects which obviously limit the magnitude of the trapped modes. Special experiments have demonstrated the existence of trapped modes in a wave tank (D. V. Evans, private communication). Moreover it is well known for TLP’s that the maximum surge exciting force occurs at a slightly smaller wavenumber than the value  $Kd = \pi$  where the phase of the incident wave is the same at both pairs of columns, suggesting that this maximum is associated with the second near-trapped mode. For large arrays it may be difficult to verify results such as those shown in Figures 5-7, due to the narrow bandwidth of the peaks and the slow rise time of such effects in an experiment of finite duration. Nevertheless

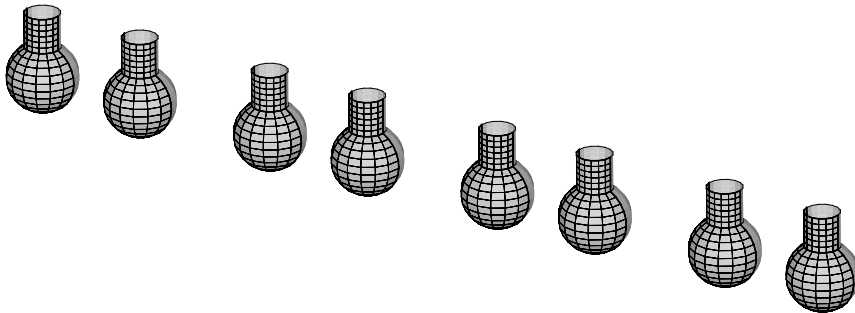


Fig. 4 Perspective view of the array  $N = 8$  with unequal spacing between adjacent elements.

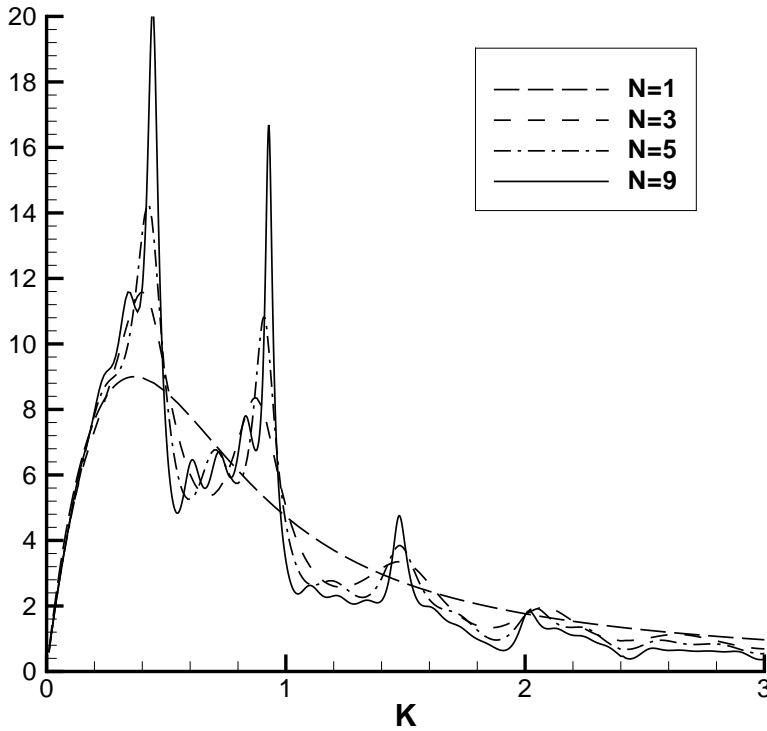


Fig. 5 Horizontal exciting force on the middle element of an equally-spaced array with  $N = 1, 3, 5, 9$  elements.

it seems prudent to consider this phenomenon carefully in the practical design of structures supported by multiple columns.

Illustrative results will be shown here for arrays of  $N$  elements which are non-cylindrical, as shown in Figure 4. Each element is defined by a circular cylinder with vertical axis and radius  $R_c$ , extending from the free surface down to the depth  $z = -D$  where a sphere of larger radius  $R_s$  is joined to the cylinder. For the results shown here  $D = R_s = 2R_c$ .

Figures 5-6 show the horizontal exciting force acting on one element of the array, normalized by the density, gravity, wave elevation, and  $R_c^2$ . The wavenumber  $K$  is normalized by  $R_c$ . The incident-wave direction is parallel to the array.

In Figure 5 results are compared for the force on the middle element in an array with  $N = 1, 3, 5, 9$  equally-spaced elements. The spacing between the axes of adjacent elements is equal to  $2\pi R_c$ . For  $N > 1$  the force tends toward a sequence of sharp peaks when  $K$  times the spacing is slightly less than  $\pi$  times an integer. As  $N$  increases the peak values increase.

Figure 6 shows the force on the fourth element of the array with  $N = 8$  elements

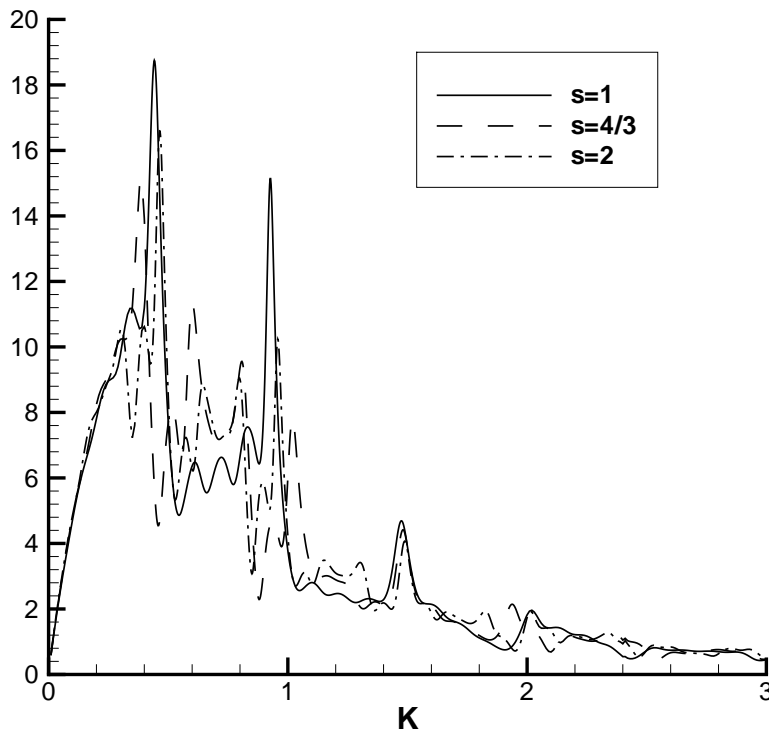


Fig. 6 Horizontal exciting force on the 4th element of the array shown in Figure 4. In the case represented by the solid line ( $s = 1$ ) the spacing is uniform. In the other cases the spacing between alternate pairs of elements is increased by the factor  $s$ .

spaced unequally, as shown in Figure 4. The spacing  $2\pi R_c$  is used between the element pairs (1,2), (3,4), (5,6), and (7,8), but this is increased by the factor  $s$  between the elements (2,3), (4,5), and (6,7). Computations are shown for  $s = (1, 4/3, 2)$ . In the first case ( $s = 1$ ) the spacing is uniform. Some reduction in the peak forces is apparent in the other cases, especially for the first Dirichlet mode just below  $K R_c = 1$ , but elsewhere the reduction is modest. Increased secondary peaks are apparent in the intermediate regime  $1/2 < K R_c < 1$ , which may be attributed to the fact that the array shown in Figure 4 is periodic with respect to four pairs of elements. Thus it is not clear that adopting a nonuniform spacing for long arrays of elements is a useful scheme to reduce the loads associated with nearly-trapped modes. On the other hand Evans & Porter [11] show a substantial reduction for a circular array with four elements when the radius of one element is increased slightly. This apparent contradiction may be due to the fact that their symmetric array is more highly-tuned, compared to the straight array with eight

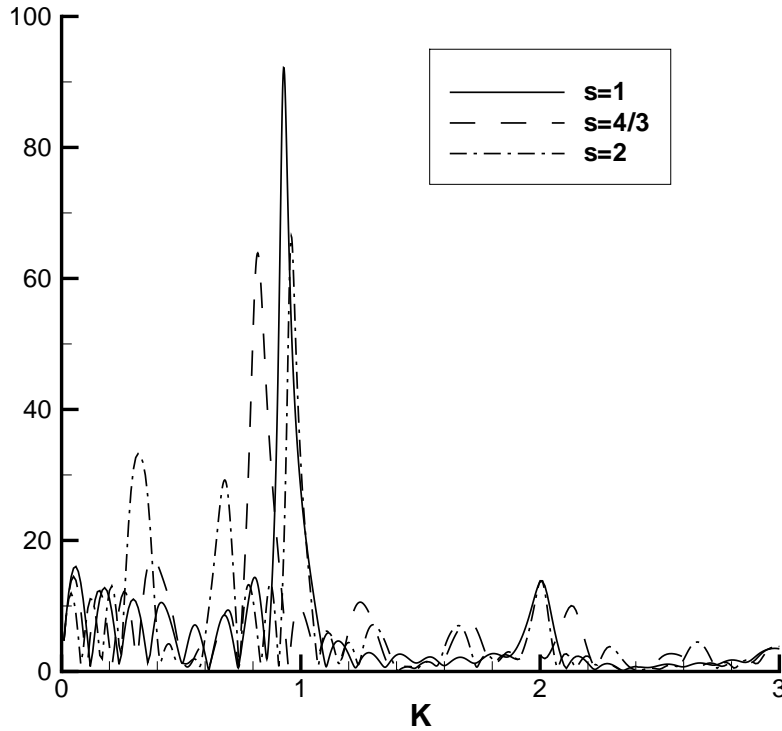


Fig. 7 Total horizontal exciting force on the complete array shown in Figure 4. Other definitions are the same as in Figure 6.

elements.

Figure 7 shows the total horizontal exciting force acting on the same array. The Neumann modes have a relatively weak influence here, due to the phase difference between adjacent elements of the array. Conversely, the Dirichlet modes, which are nearly in phase at adjacent elements, combine to give a very large exciting force just below  $Kd = \pi$ .

## 7. Second-order analysis of arrays

Malenica *et al* [32] have extended the interaction method of Linton & Evans to second order in the perturbation expansion. This is motivated by the importance of second-order wave loads and runup on multi-column structures such as TLP's, and also by the need for accurate solutions of the second-order potential as a basis for the analysis of third-order loads. Computations are presented for arrays of two, three, and four cylinders, equally spaced around a circle. Comparisons of various hydrodynamic parameters with the corresponding results for a single cylinder demonstrate the importance of accounting for the hydrodynamic interac-

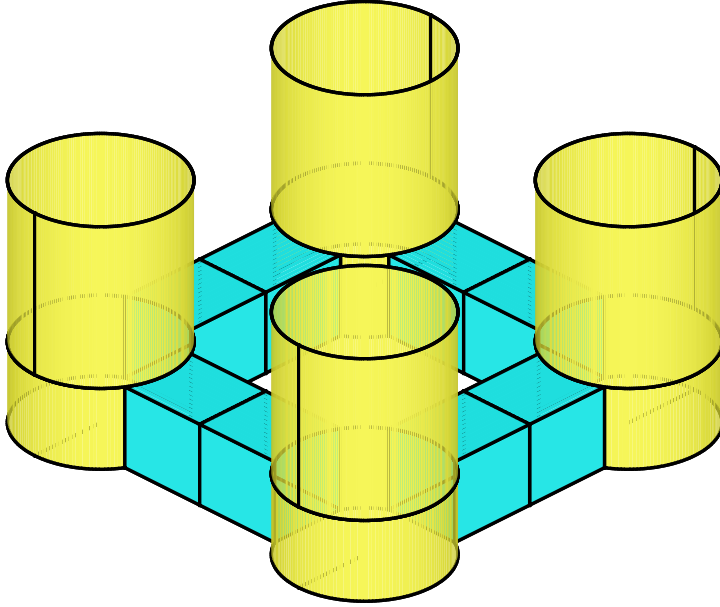


Fig. 8 Perspective view of the TLP geometry used for the comparison of the second-order free-surface elevations shown in Figure 9. The four columns have radius  $a$  and draft  $3a$ , with spacing  $4a$  between the axes of adjacent columns. The pontoons have square sections of width  $a$ .

tions, especially in the vicinity of wavenumbers where near-trapping occurs. The second-order pressure, which is known to decay slowly with depth, is particularly strong on the upwave cylinders due to the greater partial-standing-wave effect associated with reflection from the downwave cylinders. Near-trapping is shown to play a strong role, not only for the first-order solution but also for the second-order solution when the second-harmonic of the wave frequency coincides with the frequency of a trapped mode.

To illustrate the role of near-trapping, Malenica *et al* [32] present results for the first- and second-order free-surface elevations at wavenumbers where the near-trapped modes are excited directly by the first-order incident wave, and indirectly by forcing at the second-harmonic frequency. These results are for an array of four cylinders of radius  $a$ , centered at the corners of a square with sides  $4a$  and extending to the bottom in a fluid of depth  $3a$ . For that configuration and water depth the first-order trapped mode occurs at  $ka = 1.66$  and the second-harmonic forcing of the same wavenumber occurs when  $ka = 0.468$ , where  $k$  is the finite-depth



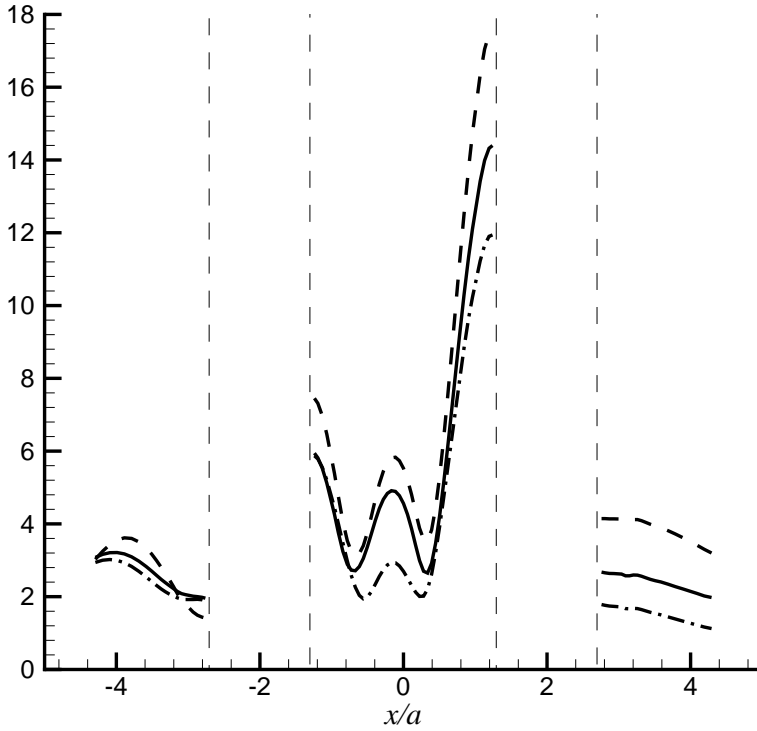


Fig. 9 Comparisons of the normalized second-order wave elevation  $|\eta_2|/kA^2$  along the diagonal line  $x = y$  connecting the centers of opposite columns of the TLP shown in Figure 8. Here  $\eta_2$  is the second-order component of the elevation,  $k$  is the wavenumber of the first-order solution, and  $A$  is the incident-wave amplitude. The incident-wave direction is parallel to the same diagonal. The positions of the columns are outlined by the vertical dashed lines. The second-order wavenumber corresponds to the first near-trapped mode. The three geometrical configurations are: (---) four bottom-mounted cylinders considered by Malenica *et al* [32], (—) the complete TLP with pontoons shown in Figure 8, and (- - -) four truncated cylinders with the same draft as the TLP.

wavenumber. In the later case the second-order runup is very large, especially on the downwave cylinder, as shown by the dashed line in Figure 9.

Similar results can be expected for a TLP, but a quantitative comparison is required to verify the use of the simpler bottom-mounted cylinders considered by Malenica *et al* [32]. For this purpose computations have been made for the TLP shown in Figure 8, and for an array of four truncated cylinders without the pontoons, both in infinite water depth. In all three configurations the radius, spacing, and depth of the cylinders or columns is the same. Comparison of the first-order

runup (not shown here) confirms that the results for all three configurations are practically identical, at the wavenumber  $Ka = 1.66$  where near-trapping occurs. This is not surprising, since the pontoons and column bottoms are deeper than the effective depth of the first-order velocity field. However at the wavenumber  $Ka = 0.468$ , where the frequency of the second-harmonic forcing coincides with a near-trapped mode, the effects of the pontoons and of the truncated columns are more important in the first-order solution. As a result there are significant differences between the three configurations, as shown in Figure 9. The computations for the bottom-mounted array are practically identical to the results shown by Malenica *et al* [32], with a maximum normalized second-order runup approaching 18. For four truncated cylinders with the same draft, in infinite fluid depth, the maximum second-order runup is reduced by about one-third. (Since the depth is changed, the first-order wavenumber is slightly different.) When the pontoons of the complete TLP are added, the results are intermediate between the two simpler cases. The use of four bottom-mounted cylinders exaggerates the maximum second-order runup on the TLP by about 22%.

## 8. Doubly periodic arrays

Column-supported VLFS structures are usually configured with rectangular arrays of elements which are periodic in two dimensions, say with  $M_x$  rows and  $M_y$  columns in the  $x, y$  directions, respectively. If  $M_x$  and  $M_y$  are both large, it is logical to seek a simplified solution for the fluid domain within the array, possibly coupled to the exterior via a local solution near the edges. This type of simplification was suggested by Kagemoto *et al* [19], and several different approaches have been explored subsequently.

Evans & Shipway [13] adopt a technique based on homogenization theory, where the region occupied by a rectangular array of cylinders is replaced by a homogeneous continuum. In this region the conservation equations are modified to account for the presence of the cylinders, with the implicit assumption that the cylinder radius is small compared to the spacing and wavelength. A matching procedure is used to connect this domain to the fluid regions outside the array. Clément & Pianet [6] show that similar results can be obtained by numerical measurements of the index of wave refraction through a triangular ‘prism’ consisting of up to 120 elements. Porter & Evans [54] compare the trapped mode wavenumbers obtained from the homogenization approximation with exact numerical results for a finite array.

If  $M_x \gg 1$  and  $M_y \gg 1$ , it is natural to consider the limiting case of a periodic array which extends to  $\pm\infty$  in both horizontal directions, covering the entire domain of the free surface. In this limit the conventional assumptions of wave scattering by compact bodies must be re-examined, and indeed such a problem may seem at first glance to be non-physical.

Chou [5] has studied this type of problem with the scattering due to periodic boundary conditions on the free surface or bottom. The principal result is that

waves can propagate through such an array without a change of amplitude, if the wave frequency is within certain ‘passing bands’. Conversely, if the frequency is within a ‘stopping band’, such propagation is not possible.

McIver [36] considers more specific problems where the scattering elements are circular cylinders, and determines the boundaries between the passing and stopping bands for specific configurations. Comparison is made with computations of the transmission coefficient for an array which is large but finite in one direction, analogous to the channel problem with a large number of cylinders on the center-plane. The transmission is effectively zero for wavenumbers near  $KL = \pi$ , where the spacing  $L$  between adjacent rows in the direction of propagation is close to half of the wavelength. The transmission is nearly complete for other values of  $KL \leq 2\pi$ , except for a narrow band near  $2\pi$ .

## 9. Conclusions

The analysis of wave interactions with multiple bodies is an important and active field of marine hydrodynamics. Many of the developments in this field follow as logical extensions from the seminal works of Ohkusu [44-49]. Subsequent work has been motivated by the increasing complexity of multiple-body configurations, and by the expanding range of applications. Significant extensions, generalizations, and improvements have been made in the computational methods for direct solutions, and in the parallel development of analytic methods for very large arrays. Fascinating scientific issues have emerged, including the roles of trapped modes and Rayleigh-Bloch waves, and their singular effects on various types of arrays.

Direct solutions of the linear wave radiation and diffraction problems are now practical, using the panel method with  $O(10)$  complex bodies or  $O(100)$  simple bodies. For axisymmetric bodies the multiple-scattering method provides an alternative approach with greater computational efficiency. The same methods have been extended to include second-order wave effects, where the computational costs limit the number of bodies to somewhat smaller numbers.

Current work is especially active in two principal areas: (1) accelerated numerical methods for analyzing larger numbers of bodies, including column-supported VLFS structures, and (2) asymptotic theories for the same configurations which are applicable when the number of elements is very large. It is obvious that these two complementary directions for research will be mutually beneficial.

Several other important challenges can be identified. One is to establish the appropriate physical role of near-trapping in practical applications. Others include the analysis of nonlinear phenomena which are important for multiple interacting bodies, such as ringing on arrays of columns, runup, and the estimation of the air-gap clearance under connecting decks. Slowly-varying nonlinear motions are important in marine operations involving vessels in close proximity. The tasks of coupling and uncoupling very large floating structures at sea require special consideration with respect to their relative motions, including both the first-order oscillatory components and second-order slowly-varying effects.

It is evident that this subject will continue to challenge scientists and engineers for many years in the future.

### Acknowledgment

The results shown in Figures 3, 5, 6, and 7 have been computed using the WAMIT program with exact representations of the geometry and B-spline representations of the solutions. The results in Figure 9 have been computed by Dr. C.-H. Lee, using the second-order extension of WAMIT.

### References

1. Budal, K., Theory for absorption of wave power by a system of interacting bodies, *J. Ship Research*, 21 (1977) 248-253.
2. Callan, M., Linton, C. M. & Evans, D. V., Trapped modes in two-dimensional waveguides, *J. Fluid Mech.*, 229 (1991) 51-64.
3. Chakrabarti, S. K., Response of multiple structures including interaction, Proc. 3rd Intl. Workshop on Very Large Floating Structures VLFS '99, Honolulu, 2 (1999) 795-804.
4. Chakrabarti, S., Hydrodynamic interaction forces on multimoduled structures, *Ocean Engineering*, 27 (2000) 1037-1063.
5. Chou, T., Band structure of surface flexural-gravity waves along periodic interfaces *J. Fluid Mech.*, 369 (1998) 333-350.
6. Clément, A. H. & Pianet, G., Numerical measurements of the index of wave refraction through a group of vertical cylinders, Proc. 16th Intl. Workshop on Water Waves and Floating Bodies, Hiroshima (2001).
7. Danmeier, D., Multiple-body simulations using a higher-order panel code, Proc. 13th International Workshop on Water Waves and Floating Bodies, Delft, The Netherlands (1998) 28-31.
8. Danmeier, D. G., A higher-order panel method for large-amplitude simulations of bodies in waves, Ph.D. Thesis, MIT (1999).
9. Evans, D. V., Linton, C. M. & Ursell, F., Trapped mode frequencies embedded in the continuous spectrum, *Quarterly J. of Mechanics and Applied Mathematics*, 52 (1993) 263-274.
10. Evans, D. V. & Porter, R., Trapped modes about multiple cylinders in a channel, *J. Fluid Mech.*, 339 (1997) 331-356.
11. Evans, D. V. & Porter, R., Near-trapping of waves by circular arrays of vertical cylinders, *Applied Ocean Research*, 19 (1997) 83-99.

12. Evans, D. V. & Porter, R., Trapping and near-trapping by arrays of cylinders in waves, *J. Engineering Mathematics*, 35 (1999) 149-179.
13. Evans, D. V. & Shipway, B. J., A continuum model for multi-column structures in waves, Proc. 15th Intl. Workshop on Water Waves and Floating Bodies, Caesaria, Israel (2000) 47-50.
14. Falnes, J., *Ocean waves and oscillating systems: linear interactions including wave-energy extraction*, Cambridge University Press (2001) (in press).
15. Faltinsen, O. & Michelsen, F., Motions of large structures in waves at zero Froude number, Proc. Intl. Symp. on the Dynamics of Marine Vehicles and Structures in Waves, London (1974) 91-106.
16. Ferreira, M. D., and Lee, C.-H., "Computation of second-order mean wave forces and moments in multibody interaction," Proc. 7th Intl. Conf. on Behaviour of Offshore Structures (BOSS '94), Cambridge, USA, 2, 303-313.
17. Kagemoto, H. and Yue, D. K. P., Interactions among multiple three-dimensional bodies in water waves: an exact algebraic method, *J. Fluid Mech.*, 166 (1986) 189-209.
18. Kagemoto, H., Fujino, M., Murai, M., & Zhu, T., Some efficient calculation techniques for hydroelastic analysis of a very large floating structure in waves, Proc. 2nd Intl. Conf. on Hydroelasticity in Marine Technology, Kyushu (1998) 165-176.
19. Kagemoto, H., Fujino, M., & Tingyao, Z., A new approximate technique for the hydrodynamic analyses of a huge floating structure, Proc. 10th Intl. Workshop on Water Waves and Floating Bodies, Oxford, UK (1995) 101-104.
20. Kashiwagi, M., Hydrodynamic interactions among a great number of columns supporting a very large flexible structure. Proc. 2nd Intl. Conf. on Hydroelasticity in Marine Technology, Kyushu (1998) 165-176; also *J. Fluids and Structures*, 14 (2000) 1013-1034.
21. Kashiwagi, M., Wave interactions with a multitude of floating cylinders. Proc. 15th Intl. Workshop on Water Waves and Floating Bodies, Caesaria, Israel (2000) 99-102.
22. Kashiwagi, M., Second-order steady forces on multiple cylinders in a rectangular periodic array, Proc. 16th Intl. Workshop on Water Waves and Floating Bodies, Hiroshima (2001).
23. Kim, D., Chen, L., & Blaskowski, Z., Linear frequency domain hydroelastic analysis for McDermott's mobile offshore base using WAMIT. Proc. 3rd Intl. Workshop on Very Large Floating Structures VLFS '99, Honolulu, 1, (1999) 105-113.

24. Kring, D., Korsmeyer, F. T., Singer, J., & White, J. K., Analyzing mobile offshore bases using accelerated boundary-element methods. Proc. 3rd Intl. Workshop on Very Large Floating Structures VLFS '99, Honolulu, 1, (1999) 348-357.
25. Landweber, L. & Chwang, A., Generalization of Taylor's added-mass formula for two bodies, *J. Ship Research*, 33, (1989) 1-9.
26. Lee, C.-H. and Newman, J. N., An assessment of hydroelasticity for very large hinged vessels, Proc. 2nd Intl. Conf. on Hydroelasticity in Marine Technology, Kyushu (1998) 27-36; also *J. of Fluids and Structures*, 14 (2000) 957-970.
27. Linton, C. M., A new representation for the free-surface channel Green's function, *Applied Ocean Research*, 21 (1999) 17-25.
28. Linton, C. M. & Evans, D. V., The interaction of waves with arrays of vertical circular cylinders, *J. Fluid Mech.*, 215 (1990) 549-569.
29. Linton, C. M. & Evans, D. V., The radiation and scattering of surface waves by a vertical circular cylinder in a channel, *Phil. Trans. Roy. Soc. London, A*, 338 (1992) 325-357.
30. Linton, C. M. & McIver, M., Resonances for cylinder arrays, Proc. 16th Intl. Workshop on Water Waves and Floating Bodies, Hiroshima (2001).
31. Løken, A., Hydrodynamic interaction between several floating bodies of arbitrary form in waves, Intl. Symp. on Hydrodynamics in Ocean Engineering, Trondheim (1981) 745-779.
32. Malenica, Š., Eatock Taylor, R. & Huang, J. B., Second-order water wave diffraction by an array of vertical cylinders, *J. Fluid Mech.*, 390 (1999) 349-373.
33. Maniar, H. D. and Newman, J. N., Wave diffraction by a long array of cylinders, *J. Fluid Mech.*, 339 (1997) 309-330.
34. Mavrakos, S. A., Hydrodynamic coefficients for groups of interacting vertical axisymmetric bodies, *Ocean Engineering* 18 (1991) 485-515.
35. Mavrakos, S. A. & McIver, P., Comparison of methods for computing hydrodynamic characteristics of arrays of wave power devices, *Applied Ocean Research*, 19 (1997) 283-291.
36. McIver, P., Water-wave propagation through an infinite array of cylindrical structures *J. Fluid Mech.*, 424 (2000) 101-125.
37. McIver, P., Linton, C. M. & McIver, M., Construction of trapped modes for waveguides and diffraction gratings, *Proc. Roy. Soc. London, Series A*, 454 (1998) 2593-2616.

38. McIver, P. & McIver, M., Wave-power absorption by a line of submerged horizontal cylinders. *Applied Ocean Research*, 17 (1995) 117-126.
39. Murai, M., Kagemoto, H., & Fujino, M., On the hydroelastic responses of a very large floating structure in waves *Jl. of Marine Science and Technology*, Society of Naval Architects of Japan (1999).
40. Nabors, K., Phillips, J., Korsmeyer, F. T., and White, J., Multipole and precorrected FFT accelerated iterative methods for solving surface integral formulations of three-dimensional Laplace problems. In *Domain-based parallelism and problem decomposition methods in science and engineering*, D. E. Keyes, Y. Saad, and D. G. Truhlar, eds., SIAM, Philadelphia (1995).
41. Newman, J. N., Wave effects on deformable bodies, *Applied Ocean Research*, 16 (1994) 47-59.
42. Newman, J. N., & Lee, C.-H., Boundary-element methods in offshore structure analysis, Proc. Offshore Mechanics and Arctic Engineering Conf. (OMAE), Rio de Janeiro (2001).
43. Newman, J. N., Maniar, H. D., & Lee, C.-H., Analysis of wave effects for very large floating structures, Proc. Intl. Workshop on Very Large Floating Structures, Hayama, Japan (1996).
44. Ohkusu, M., On the heaving motion of two circular cylinders on the surface of a fluid, Reports of Research Institute for Applied Mechanics, XVII, No.58, (1969) 167-185.
45. Ohkusu, M., On the motion of multihull ship in waves, *J. Society of Naval Architects of West Japan*, 40, (1970) 19-47.
46. Ohkusu, M., Wave action on groups of vertical circular cylinders (in Japanese), *J. Society of Naval Architects of Japan*, 131 (1972) 53-64.
47. Ohkusu, M., Hydrodynamic forces on multiple cylinders in waves, Proc. Intl. Symp. on the Dynamics of Marine Vehicles and Structures in Waves, London (1974) 107-112.
48. Ohkusu, M., Ship motions in vicinity of a structure, Proc. 1st Intl. Conf. on the Behaviour of Off-Shore Structures (BOSS '76), Trondheim, 1 (1976) 284-306.
49. Ohkusu, M., Wave reflection and transmission of a pile array (in Japanese), Bulletin of Research Institute for Applied Mechanics, 1982, No.57, 527-544.
50. Ohkusu, M., Hydrodynamics of ships in waves, in *Advances in Marine Hydrodynamics*, ed. M. Ohkusu, Computational Mechanics Publications, Southampton, UK (1996) 77-131.

51. Ohkusu, M. & Namba, Y., Hydroelastic behavior of a large floating platform of elongated form on head waves in shallow water Proc. 2nd Intl. Conf. on Hydroelasticity in Marine Technology, Kyushu (1998) 165-176.
52. van Oortmerssen, G., Hydrodynamic interaction between two structures, floating in waves, Proc. 2nd Intl. Conf. on Behaviour of Offshore Structures (BOSS '79), London (1979) 339-356.
53. van Oortmerssen, G., Some hydrodynamic aspects of multi-body systems, Proc. Intl. Symp. on Hydrodynamics in Ocean Engineering, Trondheim (1981) 725-743.
54. Porter, R. & Evans, D. V., Trapped modes about tube bundles in waveguides, IUTAM Symp. 2000/10 on Diffraction and Scattering in Fluid Mechanics and Elasticity, Univ. of Manchester (2000).
55. Ursell, F., On the heaving motions of a circular cylinder on the surface of a fluid, *Quarterly J. of Mechanics and Applied Mathematics*, 2 (1949) 218-231.
56. Ursell, F., Mathematical aspects of trapping modes in the theory of surface waves, *J. Fluid Mech.*, 183 (1987) 421-437.
57. Utsunomiya, T. & Eatock Taylor, R., Trapped modes around a row of circular cylinders in a channel, *J. Fluid Mech.*, 386 (1999) 259-279.
58. Utsunomiya, T., Watanabe, E. & Nishimura, N., Fast multipole method for hydrodynamic analysis of very large floating structures, Proc. 16th Intl. Workshop on Water Waves and Floating Bodies, Hiroshima (2001).
59. Williams, A. N. & Li, W., Water wave interactions with an array of bottom-mounted surface-piercing porous cylinders, *Ocean Engineering*, 27 (2000) 841-866.
60. Yeung, R. W. & Sphaier, S. H., Wave-interference effects on a truncated cylinder in a channel, *J. Engineering Mathematics*, 23 (1989) 95-117.